

Cite this: *RSC Sustainability*, 2025, 3, 5346

## Critical parameters and mechanism for hydrothermal polyethylene conversion

Johan H. van de Minkelis,<sup>a</sup> Anna E. de Waart,<sup>a</sup> Rinke M. Altink,<sup>b</sup> Ina Vollmer<sup>\*a</sup> and Bert M. Weckhuysen<sup>\*a</sup>

Hydrothermal conversion can convert plastic materials into smaller hydrocarbons with the use of supercritical water. However, the current knowledge of the process lacks detailed studies on the effects of different reaction parameters, such as temperature and the polymer-to-water ratio. In addition, a detailed analysis of all reaction product fractions is lacking. In this work, a multi-analytical study was performed using polyethylene with different molecular weights. We found that for this polymer, temperatures of 425–450 °C and reaction times of 0.5–2 h are necessary to achieve full conversion with high selectivity towards liquid hydrocarbon species. Apart from acting as a solvent and catalyst, supercritical water also acts as a reactant. The use of D<sub>2</sub>O showed that D-atoms from water molecules were present in the hydrocarbon products formed. This observation shows that hydrothermal conversion proceeds *via* a radical generation process induced by both the elevated temperature and hydrogen and hydroxyl radicals originating from water. The process with supercritical water lowers the reaction rate compared to pyrolysis at a similar temperature and suppresses the production of coke species.

Received 16th August 2025  
Accepted 19th August 2025

DOI: 10.1039/d5su00674k

rsc.li/rscsus

### Sustainability spotlight

Current recycling rates of plastic waste are low, with most of the waste being incinerated or landfilled, resulting in large quantities of CO<sub>2</sub> emissions and environmental harm. Chemical recycling offers a way to convert this waste into chemicals that can be used to produce new materials, thereby supporting plastic circularity and reducing our dependence on fossil resources. This work explores a chemical recycling technique for plastic waste to better understand the process and improve the overall quality of the product stream, thus enhancing plastic circularity. This supports several UN Sustainable Development Goals, particularly SDG 12 (Responsible Consumption and Production) by reducing waste and transforming it into new products, and SDG 13 (Climate Action) by lowering CO<sub>2</sub> emissions.

## Introduction

Plastic has become crucial for our society. This lightweight material is used in a wide variety of applications, like packaging, construction, and clothing, due to its versatility and tunable properties. Between 1950 and 2017, more than 9.2 billion tons of plastic were produced globally. The amount produced further increases by 400 Mt each year.<sup>1,2</sup> Most of these materials are fossil-based and often designed for single use, resulting in large quantities of discarded plastic. Proper waste management is necessary to process these plastic waste streams. Currently, the largest share of plastic waste is landfilled (40%), incinerated for energy recovery (14%), or released into the environment as litter (32%).<sup>3</sup> The way society currently handles plastic waste is not environmentally friendly and sustainable. Incineration emits large quantities of CO<sub>2</sub>. Littering and landfilling disrupt

ecosystems. More importantly, these methods lead to the loss of carbon materials derived from fossil-based resources, which must then be replenished.<sup>4</sup> Therefore, it is important to keep the already produced carbon materials in the production cycle. This would also decrease dependence on fossil resources and lower CO<sub>2</sub> emissions from waste management, thereby gradually shifting to alternative carbon sources to produce fully circular plastics.

Hence, to further improve the overall circularity of plastic, more focus should be placed on the development of recycling. Currently, most plastic materials are recycled *via* mechanical recycling.<sup>5</sup> In this method, plastics are shredded, melted, and reshaped into new plastic materials.<sup>6</sup> This is an effective way of recycling, as seen with polyethylene terephthalate (PET) bottles, but it requires a very clean stream of plastic. Over time, the properties of the plastic deteriorate, resulting in a lower-value waste product.<sup>7</sup> Chemical recycling of plastics, including polyethylene (PE) and polypropylene (PP), can convert plastic waste into smaller hydrocarbons that can be used to produce virgin quality plastics. Chemical recycling techniques include pyrolysis, hydrolysis, solvolysis, dissolution/precipitation and

<sup>a</sup>Inorganic Chemistry and Catalysis Group, Institute for Sustainable and Circular Chemistry, Department of Chemistry, Utrecht University, Universiteitsweg 99, 3584 CG Utrecht, The Netherlands. E-mail: i.vollmer@uu.nl; b.m.weckhuysen@uu.nl

<sup>b</sup>Brightsite/TNO, Urmonderbaan 22, 6167 RD Geleen, The Netherlands



oxidative conversion.<sup>8</sup> Pyrolysis is the most commonly researched method and is applied industrially although still at small scale. Pyrolysis can process a wide variety of feedstocks. However, the decomposition of plastics with pyrolysis requires a dry feedstock and yields a mixture of low value chemicals.<sup>9,10</sup>

A technique that resembles plastic pyrolysis is hydrothermal conversion. This method utilizes supercritical water to convert plastic into a product stream similar to pyrolysis oil, consisting of different hydrocarbon fractions. The products generated through this process are primarily a naphtha-like mixture and aromatic compounds. The naphtha-like fraction can be further upgraded to become compatible with conventional refinery processes, enabling its use as a feedstock for the production of new plastics and other fine chemicals. The aromatic compounds, specifically benzene, toluene and xylene (BTX), are considered high-value products, with applications in the manufacture of polystyrene (PS), PET, dyes, adhesives, and resins.<sup>11</sup> To maximize economic and material recovery potential, the process should be optimized to achieve high selectivity toward these desirable product streams.

Compared to pyrolysis, hydrothermal conversion has some advantages. The process does not require a dry feedstock as the conversion occurs in water.<sup>12</sup> This is advantageous for plastic waste processing in terms of energy efficiency, as the waste material is typically washed prior to treatment and subsequent drying steps are highly energy-intensive. By eliminating the need for drying, hydrothermal conversion can reduce the overall energy consumption in the process. Additionally, using water in the process is beneficial, as it is classified as a green solvent, is abundant, and is non-toxic.<sup>13</sup>

Despite its advantages, the hydrothermal process also presents certain challenges. Supercritical water is inherently corrosive, and the presence of metals in waste materials can further enhance this effect, potentially damaging the reactor system. To mitigate these risks, the use of corrosion-resistant reactor materials and feedstock pretreatment methods is essential.<sup>14,15</sup>

The promise of this process was recently shown by Peplow, who reported the first recycling plant using supercritical water in the Mura hydrothermal plastic recycling technology (Hydro-PR).<sup>16</sup> Mura showed that it is possible to convert contaminated polyolefin waste into light hydrocarbon gasses (10–15%), naphtha/distillate gas oil (40–60%), heavy gas oil (20–30%), and heavy residual oil (10–20%). The gasses are used for heating the reactor and the heavier oils are used for various chemicals or asphalt. The naphtha/distillate gas oil is used to produce new plastics and other chemicals.

The physical and chemical properties of water at different temperatures and pressures influence the outcome of the process.<sup>17</sup> Under ambient conditions, water functions as a highly polar solvent, with a dielectric constant of  $\sim 80$ . When the critical temperature and pressure are surpassed, the dielectric constant drops to a value of  $\sim 6$ , which makes the water behave like a non-polar solvent due to the loss of hydrogen bonds between water molecules.<sup>18–21</sup> The change from a polar to non-polar solvent allows smaller hydrocarbons to dissolve in supercritical water due to the similar dielectric constant, forming a homogeneous reaction mixture.<sup>22,23</sup> This

enhances the process in terms of heat transfer and diffusion.<sup>8,24</sup> Although, PE was found to melt and form liquid spherules in supercritical water, it is speculated that after initial breaking of C–C bonds in the polymer chains, the intermediates formed can dissolve and be further cleaved faster due to enhanced heat transfer and diffusion of products away from the reaction.<sup>22,25</sup> Upon returning to ambient conditions, the water becomes polar again and water and hydrocarbons separate, forming a two-phase system, with low mutual solubility, which can easily be separated to recover the products from the reaction mixture.

Additionally, depending on the temperature and pressure, water can catalyze different types of chemical reactions.<sup>26</sup> With increasing temperature and pressure, the formation of  $H^+$  and  $OH^-$  ions increases, thus increasing the ionic product.<sup>27</sup> Therefore, acid–base reactions are catalyzed. However, when surpassing the supercritical point, the density of water drastically drops. This decreases the ionic product formation as fewer ions can be dissolved.<sup>20</sup> Under these conditions, free radical reactions are catalyzed.<sup>28</sup> By operating under specific conditions, either acid–base or radical reactions are favored.

Only limited information on this type of chemical reaction of polyolefins in water is available in the literature. The group of Škerget has previously investigated the hydrothermal conversion of virgin and recycled high density polyethylene (HDPE), low density polyethylene (LDPE), and PP.<sup>12,29–31</sup> They aimed to recover products that can be used as fuel. Therefore, they focused on properties like the calorific value and high heating value, while lacking a deeper investigation into the composition of the different product fractions, such as the gas, liquid, wax, and water fraction. More research has been performed by Williams *et al.* and Wang *et al.*, who obtained mainly oily products ( $>90$  wt%) from PE and PP after reaction at 425 °C or above for several hours using different plastic-to-water ratios.<sup>32,33</sup> Again, the authors focus on obtaining a product, which has fuel-like properties.

While there have been multiple investigations on hydrothermal conversion, comparing these is difficult. Different studies have been performed with different experimental setups, starting materials, and conditions. Additionally, the analytical techniques applied to the different product fractions are not comparable. Besides this, the determination of the product fractions differs, as most authors determine the liquid and solid yield by weight, and calculate the gas yield by subtracting the solid yield from 100%.<sup>12,29–32</sup> Other groups calculate the gas yield with the ideal gas law and weigh the solid remainder, but do not weigh the liquid fraction.<sup>33</sup>

The above discussion shows a gap in the current knowledge of the hydrothermal conversion of PE and PP. Hence, our study focuses on the investigation of the effects of different parameters – such as temperature, reaction time, polymer-to-water ratio, molecular weight of the plastic, and plastic type (PP vs. PE) – through a detailed analysis of all reaction product fractions formed. By doing so, we obtained a more complete and consistent dataset, which provides the tools for tuning the (super-)critical parameters to obtain the desired product fractions. These tools are useful for further implementation of chemical recycling of polyolefins using supercritical water.



Furthermore, the specific role of water is investigated. It has been stated that water acts as a solvent, catalyst and/or reactant, but its role is still debatable.<sup>33–40</sup> Previous studies suggest that water is not incorporated into hydrocarbon products *via* hydrogen transfer during hydrothermal processes.<sup>33,34,39,40</sup> However, other reports using Fourier-transform infrared (FT-IR) spectroscopy have demonstrated deuterium incorporation during the upgrading of shale oil or vacuum residue.<sup>37,38</sup> These inconsistent findings, combined with the use of different probe molecules, leave the role of water in hydrothermal PE conversion uncertain. In this work, we aim to clarify this role using deuterated water as a reactant and analysing the products with <sup>2</sup>H nuclear magnetic resonance spectroscopy (NMR), mass spectrometry (MS), and FT-IR spectroscopy.

## Results and discussion

Hydrothermal conversion of PE was performed in a 50 ml high-temperature/high-pressure Parr autoclave. The PE used was a LDPE (Sigma Aldrich) with a number average molecular weight ( $M_n$ ) of 1800 g mol<sup>-1</sup> and a weight average molecular weight ( $M_w$ ) of 4000 g mol<sup>-1</sup>. Typically, the autoclave was loaded with 15 ml of ultra-pure water, an amount that was sufficient to exceed the critical pressure when heated. Depending on the experiment, a certain amount of PE was added to the autoclave, with a 1:6 polymer-to-water ratio. Prior to the reaction, the

autoclave was flushed with N<sub>2</sub> and pressurized to 5 bar N<sub>2</sub> before sealing the reactor. The reactor was heated at 5 °C min<sup>-1</sup> to above the critical temperature. A temperature of 400 °C, a reaction time of 1 h, and a pressure of 250 bar were chosen as reference conditions, based on experimental conditions commonly used in the literature, when varying the reaction parameters. At this temperature, the reaction was initiated and from this point, the reaction time was recorded. After maintaining the temperature for a set time, the reactor was cooled down to room temperature by using an ice bath. After reaching room temperature, the gaseous products were captured using a gas sampling bag. The liquid and solid products were obtained by extraction with dichloromethane (DCM) from the reaction mass and separation of the water, DCM, and solid phase. Fig. 1 shows a schematic overview of the conversion process, including the analytical approaches used to analyse the reaction product fractions formed. The degree of PE conversion is evaluated based on the increased formation of smaller hydrocarbons (*i.e.*, gaseous and liquid products) and the reduction of the wax fraction.

### Showcase of product analysis

To analyse the composition of the different reaction product fractions from hydrothermal conversion, a set of different analytical techniques was utilized (Fig. 2). The following section describes the analysis of the fractions and gives an overview on



Fig. 1 Flow scheme of the hydrothermal conversion of polyethylene (PE) and the different product fractions with representative molecules, along with the analytical methods to analyse them.



how the results were obtained. The four expected product fractions were the gaseous, DCM/oil, water, and solid phases.

Ideally, the gas phase would be quantified from the increase in pressure after the reaction at ambient temperature using the non-ideal gas law. However, due to the behaviour of small hydrocarbons under pressure, such quantification would result in significant errors. The hydrocarbons that are present in the gas phase at ambient temperatures ( $C_1$ – $C_6$ ), will (partially) liquify at elevated pressures.<sup>41</sup> This leads to a significant difference in the observed pressure increase as fewer molecules are present in the gas phase. Exact quantification of these requires knowledge of the composition and non-ideal thermodynamic behaviour of different components in the mixture. Therefore, the gaseous products were quantified using the method that is most commonly reported in the literature, which assumes that the gas yield is the remainder of the hydrocarbons after quantification of the liquid and solid phase (eqn (1)) as the process is performed in a closed system. The product distributions calculated based on the pressure difference and the non-ideal gas law are given in Fig. S1–S4.

$$\text{Gas yield (g)} = \text{starting material (g)} - \text{liquid yield (g)} - \text{solid yield (g)} \quad (1)$$

After collection, the gas fraction was analysed using gas chromatography (GC) coupled with a flame ionization detector (FID), a thermal conductivity detector (TCD) and a mass spectrometer (MS) (Fig. 2A and B). Based on this analysis, the distribution of products in the total gas fraction could be determined.

For the hydrocarbon species present in the DCM/oil phase, a set of GC techniques were applied. GC-FID was used for quantification of the oil phase. Butyl decanoate was added as an internal standard to determine the total amount of hydrocarbons present in the DCM/oil phase. To obtain the relative amounts of alkanes/alkenes and aromatics in the complex mixture of hydrocarbons, two dimensional GC coupled with MS (GCxGC-MS) was used (Fig. 2C).

The amount of solid fraction recovered depended on the experimental conditions, as in some experiments no solid material was found to be present. The solid phase was identified as a wax consisting of long chain hydrocarbons that did not dissolve in DCM. A combination of Fourier-transform infrared (FT-IR) spectroscopy (Fig. 2D), differential scanning calorimetry (DSC) (Fig. 2E) and diffusion-ordered spectroscopy (DOSY) <sup>1</sup>H nuclear magnetic resonance (NMR) (Fig. 2F) was used to determine the functionalities present in these hydrocarbons and their chain length.

The water fraction was analysed by high-performance liquid chromatography (HPLC) (Fig. S17). The analysis showed that no significant amount of carbon products was present in this phase, and therefore, the analysis is not described in detail. In the following sections, we use the analytical toolbox described above to analyse the products that were formed during the hydrothermal conversion of PE under different conditions.

### Effect of temperature

Increasing the reaction temperature from 400 °C to 450 °C resulted in an increase in conversion, as no wax was observed at

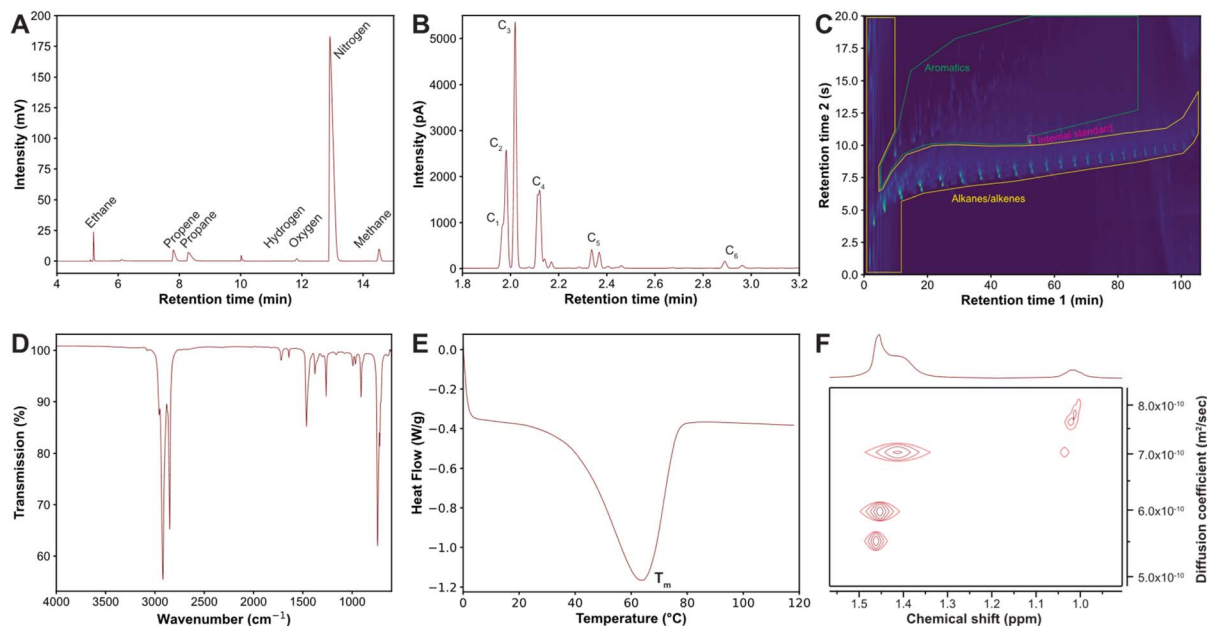


Fig. 2 Overview and examples of the analytical techniques used to investigate the composition and properties of the different product fractions obtained after the hydrothermal conversion of polyethylene (PE). Gas chromatography (GC) coupled with (a) a thermal conductivity detector (TCD) and (b) a flame ionization detector (FID) for the analysis of the gaseous products, (c) two dimensional gas chromatography coupled with mass spectrometry (GCxGC-MS) for the analysis of the hydrocarbons present in the dichloromethane (DCM)/oil phase, (d) Fourier-transform infrared (FT-IR) spectroscopy, (e) differential scanning calorimetry (DSC), and (f) diffusion-ordered spectroscopy (DOSY) <sup>1</sup>H nuclear magnetic resonance (NMR) of the solid residue collected after the hydrothermal conversion.



the highest temperature (Fig. 3). This shows that the long polymer chains are converted into smaller compounds ranging from  $C_1$ – $C_{30}$ . The oil yield increased to 31 wt% at 425 °C and 24 wt% at 450 °C compared to 11 wt% at 400 °C. The decrease at 450 °C is ascribed to further cracking of the hydrocarbons producing more gaseous compounds (34 wt% vs. 68 wt%). In the gaseous phase, an increase in smaller hydrocarbons like methane, ethane, and propane was observed, due to additional cracking reactions. In the liquid phase, 6 wt% aromatics were present at 450 °C. The increase in temperature favours the formation of aromatics, as more cyclization, dehydrogenation, and aromatization occurs, as also reported in the literature.<sup>36</sup> Regarding the solid wax products at 400 °C and 425 °C, comparing the product to the starting material using FT-IR spectroscopy, new peaks related to aromatic and unsaturated carbon bonds are found (Fig. S10). Also the  $CH_2/CH_3$  ratio decreases from 7.1 to 3.4, indicating shorter hydrocarbon chains. Carbon chain shortening is also observed with DSC, as evidenced by the decrease in melting temperature (Fig. S12). Based on the DOSY  $^1H$  NMR technique, the waxes consist of hydrocarbons with a  $M_w$  between 500 and 1200  $g\ mol^{-1}$  (Fig. S14). The changes in product composition can be attributed to differences in the properties of the supercritical fluid. As the temperature increases, the density, dielectric constant, and ionic product decrease further. This stimulates more radical reactions and enhances the heat and mass transfer during the process, thereby increasing the reaction rate.<sup>24,28</sup>

### Effect of reaction time

Increasing the reaction time has a similar effect on conversion as increasing the reaction temperature, and the two parameters are often correlated in their influence on the reaction outcome (Fig. 3). Due to the longer residence time of PE in supercritical water, more cracking reactions occur and the hydrocarbons are converted into smaller liquid and gaseous hydrocarbons. This is evident from the decrease in wax from 53 wt% after 1 h to 21 wt% after 3 h. Simultaneously, the gas and oil fractions increased by 18 wt% and 13 wt% respectively. In the gas phase, the selectivity increased for the smaller hydrocarbons, namely methane and ethane, while in the liquid phase more aromatics were observed. These findings indicate that, as expected, the

material undergoes more reactions upon increased residence time. For the remaining waxes, the  $CH_2/CH_3$  ratio was similar across different reaction times, with values varying between 3.0 and 3.8, indicating that the chain length of the hydrocarbons was similar (Fig. S10). This is further confirmed by DSC, which shows similar melting temperatures, and DOSY  $^1H$  NMR, which shows that the hydrocarbons present in the waxes had a  $M_w$  between 500 and 1150  $g\ mol^{-1}$  for all materials (Fig. S12 and S14).

### Effect of the polymer-to-water ratio

Using a higher polymer-to-water ratio resulted in similar gas yields (30–40 wt%), an increase in liquid products (9 wt% to 31 wt%) and a decrease of wax products (53 wt% to 38 wt%) (Fig. 3). The selectivity toward  $C_3$  and  $C_4$  components remained the highest, with a decrease in smaller components in the gas phase and alkanes/alkenes in the liquid phase. The relative increase in overall conversion is attributed to the availability of water to the polymer material. With less polymer material present, the contact between water and polymer increases and therefore more energy and hydrogen and hydroxyl radicals can act on the polymer material. This increases the reaction rate and hence the polymer degradation is accelerated.<sup>19,42–44</sup> The shift towards larger hydrocarbons in the gas phase indicates a change in reaction pathways with a higher contribution from hydrogen abstraction during the degradation process.<sup>12,45</sup> The remaining wax material showed similarities across different polymer-to-water ratios (Fig. S10 and S12), with an approximate  $M_w$  between 500 and 1100  $g\ mol^{-1}$  based on DOSY  $^1H$  NMR (Fig. S14).

### Reaction optimization

After a thorough investigation of the reaction parameters in hydrothermal conversion, we optimized the reaction conditions to increase conversion and selectivity towards the desired oil phase or aromatics depending on the application. The reaction was performed at multiple temperatures, 400 °C, 425 °C, and 450 °C, with reaction times varying from 0 to 3 h. The product distributions show that a reaction temperature of 400 °C is not high enough to reach full conversion within 3 h (Fig. 3). A



Fig. 3 Overview of the product distributions after the hydrothermal conversion of polyethylene (PE) with a  $M_w$  of 4000  $g\ mol^{-1}$  at various reaction temperatures, reaction times and polymer-to-water ratios. Gaseous products are presented as fully coloured blocks, liquid products as stripes and solids as dots.





Fig. 4 Overview of the product distributions of the hydrothermal conversion of polyethylene (PE) with a  $M_w$  of 137 500  $\text{g mol}^{-1}$  at various reaction temperatures, reaction times and polymer-to-water ratios. Gaseous products are presented as fully coloured blocks, liquid products as stripes and solids as dots.

prolonged reaction time is necessary to convert the starting material into a usable product fraction, as a large part of the product is present as a wax (21 wt%). Full conversion is achieved at temperatures of 425 and 450 °C. At 425 °C, a longer reaction time results in almost no wax remaining and an increase in reaction selectivity towards products in the liquid phase with approximately 5 wt% more alkanes/alkenes and aromatics in the product mixture. Higher concentrations of alkanes/alkenes and aromatics are achieved at 450 °C with a reaction time of 15 min. It is important to note that the heating period to reach 450 °C was prolonged by 15 min and therefore the total time in the supercritical region was approximately 30 min. With this short reaction time, 41 wt% alkanes/alkenes and 6 wt% aromatics are produced. Prolonging the reaction time yields similar amounts of aromatics, but a decrease in alkanes/alkenes. The gas fraction increases, as further cracking reactions result in smaller hydrocarbons. Therefore, to achieve full conversion and high selectivity towards alkanes/alkenes and aromatics, a temperature of 425 °C for 2 h or 450 °C for 15 min is recommended. Higher temperatures/longer reaction times result in over-cracking and give a larger fraction of gaseous compounds which are less useful for recycling purposes as they are often used for heating by burning and are not processed further into new chemicals.

### Higher molecular weight polyethylene

A PE with a higher  $M_w$  of 137 500  $\text{g mol}^{-1}$  was used to investigate the process with a material that is more comparable to the polymers found in consumer plastic waste. Compared to the PE with a lower  $M_w$ , similar trends are observed with respect to the reaction temperature, time, and polymer-to-water ratio (Fig. 4, S11, S13, and S15). However, the product distribution differs. For the higher  $M_w$  PE, selectivity shifts towards longer hydrocarbon products, as a larger percentage of the products are present as wax or liquid products. This is due to the longer chain length of the starting material. Under similar reaction conditions, the hydrocarbon products are longer, compared to those from the lower  $M_w$  PE, and therefore more wax and oil products are formed. Thus, higher temperatures or longer reaction times are needed to achieve full conversion of the

starting material into a gaseous or liquid product. For the higher  $M_w$  PE, reaction conditions of 425 °C for 2 h, are found to be optimal. Full conversion is achieved, with no wax and a high yield of liquid products (60 wt%).

### Polyethylene versus polypropylene

This work focuses on the use of PE as feedstock, however, besides PE, PP represents a large share of the commodity plastics. Therefore, we compare the use of PP ( $M_n = 1900 \text{ g mol}^{-1}$  and  $M_w = 8000 \text{ g mol}^{-1}$ ) with PE ( $M_n = 1800 \text{ g mol}^{-1}$  and  $M_w = 4000 \text{ g mol}^{-1}$ ) to show the differences between the two feedstocks. For this, we used a reaction temperature of 400 °C and reaction times of 1 and 3 h. With PP as feedstock, the product distribution differs significantly as compared to PE (Fig. 5). With PE the majority of product is wax, while for PP the major product fraction is liquid hydrocarbons. Under the same reaction conditions, PP produces almost no wax, indicating a higher reaction rate producing smaller hydrocarbons. The methyl-branching of PP facilitates the formation of more stable secondary radicals compared to the primary radicals formed from PE. Therefore, breaking the C-C bond in the polymer



Fig. 5 Product distributions of the hydrothermal conversion of polyethylene (PE) and polypropylene (PP) at 400 °C for 1 and 3 h. Gaseous products are presented as fully coloured blocks, liquid products as stripes and solids as dots.



backbone of PP requires less energy.<sup>46</sup> For PP, selectivity towards C<sub>3</sub> hydrocarbons in the gas phase and alkanes/alkenes in the liquid phase is the highest. Compared to PE as feedstock, PP generates 30 wt% more alkanes/alkenes and 6 wt% more aromatics. This shows that with PP, lower temperatures or shorter reaction times can be used to reach the same conversion levels as for PE.

### Role of water in the hydrothermal conversion process

The role of water in the hydrothermal conversion process is a topic of debate in the literature. It has been suggested that water functions as a solvent, catalyst, and reactant. Whether it acts as a reactant is still uncertain as the literature has revealed contradictory results.<sup>33–40,47</sup> The literature ranges from reports stating that water does not act as a reactant to studies showing C-D vibrations with FT-IR spectroscopy when the reaction is performed in D<sub>2</sub>O. To investigate this aspect in more depth, we performed the hydrothermal conversion process with D<sub>2</sub>O and analysed the products with multiple techniques. If water functions as a reactant, deuterium atoms will be present in the hydrocarbon products, and therefore they will be isotopically labelled. Analysis using MS, <sup>2</sup>H NMR, and FT-IR spectroscopy will, in that case, show characteristic features associated with deuterium incorporation in the product molecules. Comparing hydrothermal conversion under different conditions with H<sub>2</sub>O and D<sub>2</sub>O shows (small) differences in the results of all analytical techniques. In the MS of different liquid products, for instance 1-undecene (Fig. 6A) and toluene (Fig. 6B), the intensity of peaks at higher *m/z* values increases. This is due to the heavier deuterium atoms that are present. In <sup>2</sup>H NMR, new peaks appear in the liquid products when D<sub>2</sub>O is used instead of H<sub>2</sub>O, indicating the presence of deuterium atoms in the hydrocarbon products (Fig. 6C). FT-IR spectroscopy of the liquid phase shows

new peaks related to C-D vibrations at ~2200 cm<sup>-1</sup> (Fig. 6D), which are not present when H<sub>2</sub>O is used.<sup>48</sup>

Using different reaction parameters, like a longer reaction time of 3 h or an increased reaction temperature of 450 °C, similar results are observed (Fig. 6C and D). Under all conditions, the signals are present in (very) low quantities and could only be observed with high sample concentrations for analysis. These results show that deuterium atoms are at least partially transferred from D<sub>2</sub>O to the hydrocarbons, likely through the generation of deuterium radicals that combine, during a termination step, with hydrocarbon radicals. Therefore, supercritical water functions as a reactant in the hydrothermal conversion of polyolefins.

### Elucidation of the reaction mechanism

Based on the reaction products of the hydrothermal conversion and the related analyses, a plausible reaction mechanism can be proposed, which is shown in Scheme 1. Mechanisms have already been reported in literature, but these do not include the interaction with water and the radicals that are produced.<sup>30,31,33</sup> We demonstrate that hydrogen originating from water is found in the hydrocarbons formed and that a higher water to polymer ratio results in faster conversion. Therefore, water should be included in the mechanism.

We propose that the conversion process is mainly initiated by homolytic cleavage of the hydrocarbon backbone of PE, which generates two hydrocarbon radicals, because of the properties of supercritical water at elevated temperatures, particularly its reduced ionic product. The low ionic product favours the formation of free radicals, thereby promoting homolytic bond cleavage, which is often considered as the first step in the cracking of hydrocarbon chains.<sup>28</sup> These radicals can undergo further cracking *via* β-scission to generate an unsaturated hydrocarbon and another hydrocarbon radical. This radical can undergo subsequent reactions. Under supercritical conditions, the presence of hydrogen and hydroxyl radicals can also initiate the process. These radicals can abstract a hydrogen from the PE backbone, to generate H<sub>2</sub> or water, and a hydrocarbon radical. This radical can undergo homolytic cleavage to generate a new hydrocarbon radical and an unsaturated hydrocarbon. The new radical can afterwards react *via* β-scission to generate an additional unsaturated hydrocarbon and a hydrocarbon radical, and this will continue the cleavage of the hydrocarbon backbone. Replacement of PE by PP follows the same mechanism. The reaction is initiated by the formation of the hydrocarbon radical. This requires less energy, as the hydrocarbon radical formed from PP is more stable compared to the one from PE.

The pool of unsaturated hydrocarbons can undergo a series of reactions, like hydrogenation, isomerisation, cyclization, aromatization, and gasification. These reactions produce a mixture of smaller (un)saturated and cyclic hydrocarbons, which can be present in the gaseous, liquid, or solid phase. Additionally, the unsaturated hydrocarbons can interact with hydroxyl radicals to generate oxygenated compounds, like alcohols and acids. These are present in the water phase.



Fig. 6 Hydrothermal conversion of polyethylene (PE) with H<sub>2</sub>O (red) and D<sub>2</sub>O (blue) as liquid medium. Two-dimensional gas chromatography coupled with mass spectrometry (GCxGC-MS) analysis of the liquid products, with the MS of (a) 1-undecene and (b) toluene highlighted and (c) <sup>2</sup>H nuclear magnetic resonance (NMR), and (d) Fourier-transform infrared (FT-IR) spectroscopy of reactions performed at different reaction temperatures and times.





Scheme 1 Mechanistic overview of the reactions occurring during the hydrothermal conversion of polyethylene (PE).

Furthermore, the hydrocarbon radicals produced can terminate *via* two pathways. Disproportionation of two radicals generates a saturated and an unsaturated hydrocarbon. The second possibility is by recombination of two radicals, forming a single saturated hydrocarbon. These compounds are present in the different product phases.

### Hydrothermal conversion versus pyrolysis

Hydrothermal conversion has similarities with thermal pyrolysis. Both conversion processes proceed at elevated temperatures. Polymers are converted *via* random radical reactions, generating a mixture of gaseous and liquid hydrocarbons. To compare these two processes, the pyrolysis of PE was performed using the same setup as the hydrothermal conversion to enable a 1-to-1 comparison between the two processes. The thermal pyrolysis was performed at 400 °C for 0.5 and 1 h. A significant difference between the two processes is the pressure: 250 bar for hydrothermal conversion due to the vaporization of water and only 50 bar for thermal pyrolysis caused by the formation of gaseous products. When comparing the two conversion processes, pyrolysis shows a higher reaction rate compared to the hydrothermal conversion (Fig. 7). While hydrothermal conversion generates 50 wt% wax at 400 °C for 1 h, pyrolysis generates 50 wt% gaseous products and 46 wt% liquid products. This large fraction of gaseous and liquid products indicates a high reaction rate. In the liquid phase, the selectivity is 33 wt% towards alkanes/alkenes and 11 wt% for aromatics. This is significantly more than that observed for hydrothermal conversion under similar conditions. To achieve similar reaction mixtures in both processes, the pyrolysis process can be

shortened. This increases the oil yield to 60 wt% with the highest selectivity toward alkanes/alkenes, when the reaction is performed for 0.5 h. For the hydrothermal conversion to produce a similar reaction mixture, prolonged reaction times and/or temperatures are needed, as discussed in previous sections. Under all conditions, hydrothermal conversion exhibits lower selectivity towards aromatics compared to pyrolysis. Independent of parameter variations, pyrolysis produces coke, which is never observed during hydrothermal conversion, irrespective of the reaction conditions applied. This is a characteristic of the pyrolysis reaction which can be



Fig. 7 Product distributions of the hydrothermal conversion at 400 °C for 1 h and 450 °C for 0.25 h and thermal pyrolysis at 400 °C for 0.5 h and 1 h of polyethylene (PE) with a molecular weight ( $M_w$ ) of 4000  $\text{g mol}^{-1}$ . Gaseous products are presented as fully coloured blocks, liquid products as stripes and solids as dots.



prevented through hydrothermal conversion, thereby converting PE into more usable reaction products.

The density of the reaction medium plays a critical role in the degradation behaviour of PE. In supercritical water at 250 bar, the high fluid density facilitates enhanced heat and mass transfer and promotes radical stabilization, all of which contribute to a more uniform and controlled breakdown. In contrast, pyrolysis in nitrogen at 50 bar occurs in a lower-density, inert environment, and relies primarily on random chain scission, allowing free radicals to persist and often resulting in the formation of heavier products and solid residues such as coke. These differences in reaction medium could be used as an effective tool to control the product selectivity during the degradation process of plastics.

## Conclusions

The hydrothermal conversion of polyethylene (PE) was studied *via* a multi-analytical approach to investigate the critical reaction parameters, including temperatures ranging from 400 to 450 °C and polymer-to-water ratios of 1:4 to 1:12, and their effects on the reaction product distribution and related properties. With increasing reaction temperature and time, both sets of PE materials with different molecular weights ( $M_w$ ) were converted into shorter chain hydrocarbon products, with reaction temperatures above 425 °C or reaction times up to 2 h necessary to reach full conversion of the starting material. Using less polymer compared to the amount of water, the selectivity shifted towards more gaseous products with the highest selectivity observed for C<sub>3</sub> and C<sub>4</sub> hydrocarbons. This indicates an increased reaction rate. The use of higher  $M_w$  PE material showed that the reaction products consisted of longer hydrocarbon chains and that higher temperatures or longer reaction times were needed to achieve full conversion compared to a similar polymer material with a lower  $M_w$ .

Using polypropylene (PP) instead of PE showed improved performance, as milder reaction conditions were required to fully convert the starting polymer material. Compared to a similar process, namely pyrolysis, hydrothermal conversion had a lower conversion rate due to the suppressing effect of water, but did not generate unwanted coke species.

Interestingly, by performing the hydrothermal reaction with D<sub>2</sub>O instead of H<sub>2</sub>O, it was shown that water is incorporated in the hydrocarbon products. This observation indicates that water also functions as a reactant in the hydrothermal conversion. Based on this finding, it is proposed that the reaction mechanism proceeds *via* radical formation through homolytic cleavage, induced by elevated temperatures and hydrogen abstraction by hydrogen and hydroxide radicals generated from water.

## Author contributions

J.H. van de Minkelis: conceptualization, experiments, data analysis, writing. A.E. de Waart: experiments, data analysis, review. R.M. Altink: discussion and review. I. Vollmer: supervision, conceptualization, discussion and review. B.M.

Weckhuysen: supervision, conceptualization, discussion, review, and funding acquisition. All authors have read and approved the final version of the manuscript.

## Conflicts of interest

There are no conflicts to declare.

## Data availability

The authors have cited additional references within the supporting information (SI).<sup>49,50</sup> See DOI: <https://doi.org/10.1039/d5su00674k>. All data and python scripts utilized in the manuscript have been uploaded to the Yoda repository and are available at <https://doi.org/10.24416/UU01-D8GCE4>.

## Acknowledgements

Sebastian Rejman (Utrecht University, UU) is acknowledged for the development of the python script for the GCxGC-MS data analysis. This work was supported by TNO/Brightsite and the Netherlands Organization for Scientific Research (NWO) in the framework of the Gravitation Program, MCEC (Netherlands Center for Multiscale Catalytic Energy Conversion). B.M.W and I.V. are supported by the Advanced Research Center (ARC) Chemical Buildings Blocks Consortium (CBBC), a public-private research consortium in The Netherlands ([arc-cbbc.nl](http://arc-cbbc.nl)). I.V. also acknowledges a Veni grant from NWO (VI.Veni.202.191).

## References

- 1 Plastics Europe, *The Circular Economy for Plastics – A European Analysis*, Plastics Europe, 2024, pp. 32–43.
- 2 *Plastic Atlas: Facts and Figures about the World of Synthetic Polymers*, ed. L. Fuhr and M. Franklin, Heinrich Böll Foundation and Break Free from Plastics, 2019, pp. 10–11.
- 3 Ellen MacArthur Foundation, *The New Plastics Economy: Rethinking the Future of Plastics & Catalysing Action*, The Ellen MacArthur Foundation, 2017, pp. 18–32.
- 4 A. J. Martín, C. Mondelli, S. D. JayDev and J. Pérez-Ramírez, *Chem*, 2021, 7, 1487–1533.
- 5 Z. O. G. Schyns and M. P. Shaver, *Macromol. Rapid Commun.*, 2021, 42, 2000415.
- 6 J. M. Garcia and M. L. Robertson, *Science*, 2017, 358, 870–872.
- 7 M. Shamsuyeva and H. J. Endres, *Compos., Part C: Open Access*, 2021, 6, 100168.
- 8 I. Vollmer, M. J. F. Jenks, M. C. P. Roelands, R. J. White, T. van Harmelen, P. de Wild, G. P. van der Laan, F. Meirer, J. T. F. Keurentjes and B. M. Weckhuysen, *Angew. Chem., Int. Ed.*, 2020, 59, 15402–15423.
- 9 Y. Tsuchiya and K. Sumi, *J. Polym. Sci., Part A: Gen. Pap.*, 1969, 7, 1599–1607.
- 10 M. Kumar, A. Olajire Oyedun and A. Kumar, *Renewable Sustainable Energy Rev.*, 2018, 81, 1742–1770.



- 11 Y. Wu, J. Yang, G. Wu, W. Gao, E. E. Silva Lora, Y. M. Isa, K. A. Subramanian, A. Kozlov, S. Zhang and Y. Huang, *ACS Sustain. Chem. Eng.*, 2023, **11**, 11700–11718.
- 12 M. Čolnik, P. Kotnik, Ž. Knez and M. Škerget, *J. Supercrit. Fluids*, 2021, **169**, 105136.
- 13 J. N. Jocz, L. T. Thompson and P. E. Savage, *Chem. Mater.*, 2018, **30**, 1218–1229.
- 14 B. R. Pinkard, D. J. Gorman, K. Tiwari, E. G. Rasmussen, J. C. Kramlich, P. G. Reinhall and I. V. Novosselov, *Heliyon*, 2019, **5**, e01269.
- 15 N. Ghavami, K. Özdenkçi, G. Salierno, M. B. Björklund-Sänkiaho and C. de Blasio, *Biomass Convers. Biorefin.*, 2023, **13**, 12367–12394.
- 16 M. Peplow, *Nature*, 2025, **638**, 22–25.
- 17 R. W. Shaw, T. B. Brill, A. A. Clifford, C. A. Eckert and E. U. Franck, *Chem. Eng. News Arch.*, 1991, **69**, 26–39.
- 18 T. Moriya and H. Enomoto, *Polym. Degrad. Stab.*, 1999, **65**, 373–386.
- 19 K. Jin, P. Vozka, G. Kilaz, W. T. Chen and N. H. L. Wang, *Fuel*, 2020, **273**, 117726.
- 20 S. Wang, D. Xu, Y. Guo, X. Tang, Y. Wang, J. Zhang, H. Ma, L. Qian, and Y. Li, in *Supercritical Water Processing Technologies for Environmental, Energy and Nanomaterial Application*, Xi'an Jiaotong University Press and Springer Nature Singapore Pte Ltd 2020, **1**, 2019, ch. 1 Introduction, pp. 1–3.
- 21 H. Weingärter and E. U. Franck, *Angew. Chem., Int. Ed.*, 2005, **44**, 2672–2692.
- 22 Z. Fang, R. L. Smith, H. Inomata and K. Arai, *J. Supercrit. Fluids*, 2000, **16**, 207–216.
- 23 A. D. Sen, V. G. Anicich and T. Arakelian, *J. Phys. D: Appl. Phys.*, 1992, **25**, 516–521.
- 24 S. Kraft and F. Vogel, *Ind. Eng. Chem. Res.*, 2017, **56**, 4847–4855.
- 25 G. Brunner, *J. Supercrit. Fluids*, 2009, **47**, 373–381.
- 26 P. E. Savage, S. Gopalan, T. I. Mizan, C. J. Martino and E. E. Brock, *AIChE J.*, 1995, **41**, 1723–1778.
- 27 Y. Marcus, in *Supercritical Water A Green Solvent: Properties and Uses*, Wiley, New Jersey, **1**, 2012, ch. 2 Bulk Properties of SCW, pp. 22–56.
- 28 R. O. Caniaz and C. Erkey, *Chem. Eng. Res. Des.*, 2014, **92**, 1845–1863.
- 29 M. Irgolič, M. Čolnik, P. Kotnik, L. Čuček and M. Škerget, *Chem. Eng. Trans.*, 2023, **103**, 727–732.
- 30 M. Čolnik, P. Kotnik, Ž. Knez and M. Škerget, *Polymers*, 2022, **14**, 4415.
- 31 M. Irgolič, M. Čolnik, P. Kotnik, L. Čuček and M. Škerget, *J. Clean. Prod.*, 2024, **463**, 142718.
- 32 M. Mathew, M. A. Nahil, A. B. Ross and P. T. Williams, *Energy Fuels*, 2024, **38**, 12810–12823.
- 33 W. T. Chen, K. Jin and N. H. L. Wang, *ACS Sustain. Chem. Eng.*, 2019, **7**, 3749–3758.
- 34 G. Popelier, G. Dossche, S. P. Kulkarni, F. Vermeire, M. Sabbe and K. M. van Geem, *J. Anal. Appl. Pyrolysis*, 2024, **183**, 106805.
- 35 N. I. Ahamed Kameel, W. M. A. Wan Daud, M. F. Abdul Patah and N. W. Mohd Zulkifli, *Energy Convers. Manage.:X*, 2022, **14**, 100196.
- 36 P. Zhao, Z. Yuan, J. Zhang, X. Song, C. Wang, Q. Guo and A. J. Ragauskas, *Sustain. Energy Fuels*, 2021, **5**, 575–583.
- 37 R. Djimasbe, M. A. Varfolomeev, N. M. Khasanova, A. A. Al-Muntaser, R. R. Davletshin, M. A. Suwaid and G. Z. Mingazov, *J. Supercrit. Fluids*, 2024, **204**, 106092.
- 38 M. Hosseinpour, S. Fatemi and S. J. Ahmadi, *J. Supercrit. Fluids*, 2016, **110**, 75–82.
- 39 T. Xu, Z. Liu and J. Wu, *Energy Fuels*, 2013, **27**, 3148–3153.
- 40 M. Morimoto, Y. Sugimoto, Y. Saotome, S. Sato and T. Takanohashi, *J. Supercrit. Fluids*, 2010, **55**, 223–231.
- 41 Gas Encyclopedia by Air Liquide, <https://encyclopedia.airliquide.com>, accessed April 2025.
- 42 B. Bai, H. Jin, C. Fan, C. Cao, W. Wei and W. Cao, *Waste Manag.*, 2019, **89**, 247–253.
- 43 Y. Liu, K. Chandra Akula, K. Phani Raj Dandamudi, Y. Liu, M. Xu, A. Sanchez, D. Zhu and S. Deng, *Chem. Eng. J.*, 2022, **446**, 137238.
- 44 H. Jin, B. Bai, W. Wei, Y. Chen, Z. Ge and J. Shi, *ACS Sustain. Chem. Eng.*, 2020, **8**, 7039–7050.
- 45 Y. Miao, A. von Jouanne and A. Yokochi, *Polymers*, 2021, **13**, 449.
- 46 J. McMurry, in *Organic Chemistry: A Tenth Edition*, OpenStax, Houston, 2023, ch. 7: Alkenes: Structure and Reactivity, pp. 207–242.
- 47 Z. Chen, *Fuel*, 2024, **366**, 131380.
- 48 A. Sattler, *ACS Catal.*, 2018, **8**, 2296–2312.
- 49 R. Evans, Z. Deng, A. K. Rogerson, A. S. McLachlan, J. J. Richards, M. Nilsson and G. A. Morris, *Angew. Chem., Int. Ed.*, 2013, **52**, 3199–3202.
- 50 R. Evans, G. Dal Poggetto, M. Nilsson and G. A. Morris, *Anal. Chem.*, 2018, **90**, 3987–3994.

